Gastrointestinal Stromal Tumor (GIST): Computed Tomographic Features and Correlation of CT Findings with Histologic Grade

Siriporn Pinaikul MD*, Piyanoot Woodtichartpreecha MD*,
Samornmas Kanngurn MD**, Sombat Leelakiatpaiboon MSc***

** Division of Diagnostic Imaging, Department of Radiology, Faculty of Medicine, Prince of Songkla University, Songkhla, Thailand*
*** Department of Pathology, Faculty of Medicine, Prince of Songkla University, Songkhla, Thailand*
**** Division of Radiotherapy, Department of Radiology, Faculty of Medicine, Prince of Songkla University, Songkhla, Thailand*

Objective: *To characterize the CT features and to identify predictors of malignancy from CT of GISTs.*
Material and Method: *A retrospective review of CT images of 50 patients with pathologically and immunohistochemically proven GISTs was done by two radiologists and final interpretations were reached by consensus. Images were evaluated for site, size, contour, boundary, growth pattern, enhancement pattern, degree of enhancement, necrosis, calcification, ulceration, perilesional fat stranding, evidence of bowel obstruction, and signs of malignancy. Categorical variables were compared using Fisher's exact test and continuous variables used the t-test. Univariate and multivariate logistic regression models were used to identify significant predictors of a high mitotic rate.*
Results: *Of the 50 patients, the most common location of GISTs was stomach (62%) The mean size was 10.2 cm (SD 5.2 cm). The contour was lobulated in 84%. The boundary was smooth in 84%. The growth pattern was exophytic in 68%. Most of tumors had heterogeneous density on post-contrast images (88%). Necrosis (84%), calcification (14%), ulceration (40%), perilesional fat stranding (44%), and bowel obstruction (2%) were present in the tumors. The CT signs of malignancy found were adjacent organ invasion (18%), ascites (18%), lymphadenopathy (6%), liver metastasis (20%), and peritoneal seeding (16%). Necrosis and peritoneal seeding were statistically significant independent predictors for high mitotic GISTs in multivariate logistic regression ($p<0.05$). The probability of a high mitotic rate was 1 (95% CI, 0.40-1.00) in the presence of both necrosis and peritoneal seeding.*
Conclusion: *The stomach was the most common site of GIST. The CT features of GIST were lobulated, smooth tumor margins, exophytic growth pattern, and heterogeneous enhancement on post-contrast CT images. Presence of both necrosis and peritoneal seeding were found to be a significant predictor of high mitotic rate of GISTs. The probability of a high mitotic rate was 1 (95% CI, 0.40-1.00).*

Keywords: *Computed tomography, Gastrointestinal stromal tumor (GIST)*

J Med Assoc Thai 2014; 97 (11): 1189-98
Full text. e-Journal: *http://www.jmatonline.com*

Gastrointestinal stromal tumors (GISTs) are rare but are the most common mesenchymal neoplasms of the gastrointestinal tumors. In the past, these tumors were classified as smooth muscle tumors, leiomyomas, leiomyosarcomas, and leiomyoblastoma, because they were believed to be derived from smooth muscle layers of the gastrointestinal tract. Until 1983, electron microscopy and immunohistochemistry findings revealed lack of smooth muscle and nerve sheath cells[1,2]. Currently, the best defining feature of GISTs is a positive expression of KIT (CD 117), a tyrosine kinase growth factor receptor. GISTs are believed to be derived from interstitial cells of Cajal[3,4]. The most common site of GISTs is the stomach (70%), followed by small intestine (20%), colon and rectum (5%), and esophagus (<5%)[5].

The computed tomographic findings of GISTs have been previously described in the literatures[6-10] and showed some distinctive features that help differentiate them from epithelial neoplasms[7]. However, only a few studies have attempted to correlate CT features with the histologic grading or prediction of malignancy and they have produced conflicting results. Tateishi et al[11] reported that an extrinsic epicenter and an unclear boundary were the most significant predictors of high-grade GISTs,

Correspondence to:
Pinaikul S, Division of Diagnostic Imaging, Department of Radiology, Faculty of Medicine, Prince of Songkla University, 15 Kanchanavanit Road, Hat Yai, Songkhla 90110, Thailand.
Phone: 074-451-501, Fax: 074-429-925
E-mail: doctorjurn@yahoo.com

whereas Kim et al[12] and Yang et al[13] found that only large tumor size had predictive value with respect to malignant GISTs. Ulusan et al[14] reported that lesion size larger than 5 cm, heterogeneous enhancement, tumor location (stomach), metastases, and necrotic component were significantly more frequent in high mitotic index GISTs.

The purposes of the present study were to describe the CT features of GISTs and to determine whether some CT characteristics were useful to predict malignancy of these tumors.

Material and Method

Patients

The medical records of 90 patients with histological and immunohistochemical diagnosis (CD117-positive) of GIST in our institution between January 2006 and March 2011 were reviewed. Forty patients whose CT scans were not available were excluded from the study. Thus, fifty patients were enrolled in the present study for reviewing their CT images. Clinical data including sex, age and presenting symptoms were also recorded. Eleven patients whose pathological specimens were obtained from biopsy and two patients who received imatinib mesylate treatment before surgical resection were excluded from the analysis of association between each CT feature and mitotic status (Fig. 1). The study was approved by the Institutional Review Board of Songklanagarind Hospital.

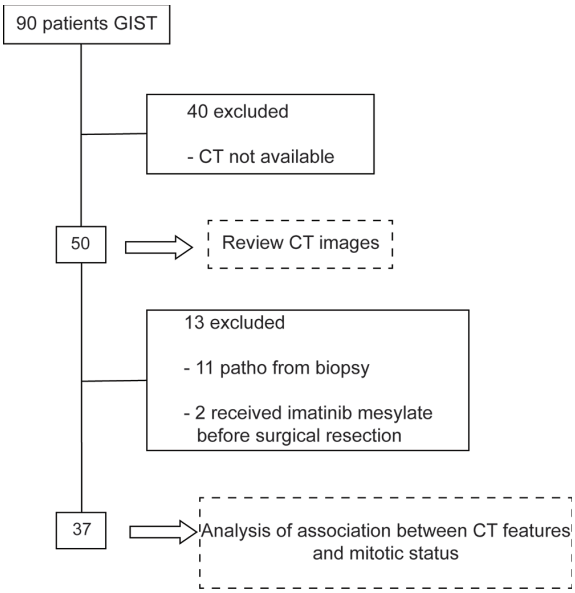

Fig. 1 Flow diagram of the study patients.

CT techniques

In 50 patients, CT examinations were performed using the Tomoscan AVI (Philips Medical Systems, n = 29) single-detector helical CT scanner, or the Brilliance 64 (Philips Medical Systems, n = 21). All patients received 800 ml of diluted oral contrast material routinely for one hour and 300 ml of oral water immediately before undergoing scanning. Each patient received 2ml/kg of nonionic contrast material. The contrast material was injected by automatic injector at a rate of 2.5 ml/sec in the single-detector scanner and at a rate of 3.5 ml/sec in the Brilliance 64 scanner. Scanning parameters of the Tomoscan AVI were 7-mm collimation, 7-mm reconstruction interval, 1.42 table pitch, and 1.0 sec rotation time. If a Brilliance 64 scanner was used, the parameters were 3-mm slice thickness, and 2-mm reconstruction interval, 0.75 seconds of rotation, pitch of 0.641, and 34.2 mm/sec table speed.

In 26 patients, biphasic CT scans were obtained at 25 to 30 seconds delay for arterial phase of upper abdomen, and at 60 to 70 seconds delay for portal venous phase of whole abdomen after initiation of contrast material injection. In 24 patients, monophasic CT scans were obtained at 60 to 70 seconds scan delay (portal venous phase). Unenhanced studies were obtained in 46 patients.

Image analysis

Two radiologists, who were blinded from the histologic result, reviewed the CT images retrospectively and independently. Initial disagreement between radiologists regarding CT characteristics range from 2% (for obstruction) to 16% (for difference in necrosis of two or more grades). Limits of agreement (95% of measurements) for tumor size were -1.5 cm to 1.8 cm; three images resulted in size differences of -2.9, 1.9, and 3.5 cm. Final interpretation was reached by consensus. All CT images were reviewed from the picture archiving and communication system (PACS). The CT scans were reviewed to determine site, size, contour, boundary, growth pattern, enhancement pattern, degree of enhancement, necrosis, calcification, ulceration, and perilesional fat stranding.

The size was measured in the greatest dimension on venous phase. Tumor contour was defined as round, ovoid, or lobulated. The boundary was classified as smooth, irregular, or combined. The growth pattern was categorized as endoluminal, exophytic, or mixed. Endoluminal growth pattern was defined if the tumor was completely confined to the

bowel lumen without bulging into the extraluminal space. Exophytic growth pattern referred to a mass confined to the extraluminal space without bulging into the bowel lumen. Mixed growth pattern was defined as a dumbbell appearance. Enhancement pattern was subjectively categorized as homogeneous and heterogeneous enhancement. The degree of enhancement of the soft-tissue portions of a tumor was evaluated against that of the muscle and liver: poor enhancement, identical to or less than that of the muscle; moderate enhancement, more than that of the muscle and less than that of the liver; and good enhancement, identical to or more than that of the liver. The degree of tumor necrosis was evaluated subjectively and classified as absent, mild (<30% necrosis of the tumor), moderate (between 30% to 70% necrosis of the tumor), and severe (>70% necrosis of the tumor). Ulceration was considered present if there was fluid, gas, or oral contrast material in the focal defect inside the mass.

Evidence of invasion to the adjacent organ, ascites, distant metastasis, lymphadenopathy, and evidence of bowel obstruction were also evaluated and recorded. Lymphadenopathy was considered present if a lymph node greater than 1 cm in the short axis was observed.

Histologic analysis

The histologic grading was reviewed by an experienced gastrointestinal pathologist and classified into two groups: low mitotic rate (no more than 5 mitotic counts per 50 high-power fields) and high mitotic rate (more than 5 mitotic counts per 50 high-power fields).

Statistical analysis

There have been many risk scores for malignancy of GISTs published to date[15-19], but all have been based on a combination of size, mitotic rate, and location of tumor. While tumor size and site can be generally evaluated on CT scan. The authors evaluated the correlations between each CT feature and mitotic rate.

Categorical variables were compared using chi-square test or Fisher's exact test as appropriate and continuous variables using the t-test. The level of significance used for inclusion in the model in multivariate logistic regression was less than 0.20. The multivariate logistic regression model was used to identify significant predictors of a high mitotic rate. The model was refined by sequential backward removal of variables not contributing significantly to the fit of the model, based on change in log likelihood of successive models. Tissue characteristics showing evidence of relationship with mitosis status were selected and combinations of these characteristics tabulated against mitosis status. A predictive probability and 95% confidence interval for high mitosis in our samples were calculated for each combination. A logistic regression model incorporating the Firth bias reduction modification to account for zero cells was constructed using the combination variable as the predictor. A p-value <0.05 was considered as statistically significant difference. The statistical analysis was performed using Stata 7 and R 2.14.0.

Results

Of the 50 patients, 25 were male (50%). The age range of study patients was 11 to 82 years (mean age 60, SD 11 years). The most common presenting symptoms were gastrointestinal bleeding in 17 patients (34%), followed by abdominal pain in 15 patients (30%), palpable abdominal mass in eight patients (16%), bloating in three patients (6%), bowel habit change in one patient (2%), hemoptysis in one patient (2%), and obstructive jaundice in one patient (2%). Tumors were incidentally detected on CT performed for clinical indications for other diseases in four patients (8%) who were asymptomatic. Thirty-one tumors (62%) occurred in the stomach, 17 (34%) in the small bowel, and two (4%) in the rectum. In those tumors located in the small bowel, four were in the duodenum, six in the jejunum, and seven in the ileum (Table 1).

The patients' CT characteristics were shown in Table 2. The size of the tumors ranged from 1.2 to 22.6 cm (mean 10.2, SD 5.2 cm). Lobulated contour and smooth boundary were each shown by 42 tumors (84%). Most GISTs (34 tumors, 68%) showed exophytic growth pattern (Fig. 2) and heterogeneous enhancement pattern (44 tumors, 88%). Necrosis (Fig. 3) was found in 42 tumors (84%). Only one patient showed evidence of gut obstruction from a large 17-cm tumor located in the rectum.

Eighteen patients (36%) had metastatic lesions to the liver or peritoneum (Fig. 3) at the time of presentation on CT scans, three patients had both liver and peritoneal metastases, seven had only liver metastases, and five had only peritoneal metastases. The attenuation of metastatic hepatic nodules on portal venous phase was lower than that of the normal surrounding parenchyma in nine patients. Two metastatic nodules in one patient showed isoattenuation

Table 1. General characteristics of patients

Characteristics	Number (%) Total n = 50
Gender	
Male	25 (50)
Female	25 (50)
Age (year), mean ± SD	60±11
Presenting symptoms	
Gastrointestinal bleeding	17 (34)
Abdominal pain	15 (30)
Palpable abdominal mass	8 (16)
Bloating	3 (6)
Bowel habit change	1 (2)
Hemoptysis	1 (2)
Obstructive jaundice	1 (2)
Asymptomatic	4 (8)
Lesion location	
Stomach	31 (62)
Small bowel	17 (34)
Rectum	2 (4)

Table 2. CT findings of GISTs in 50 patients

Characteristics of CT finding of GISTs	Number (%) Total n = 50
Size	
≤5 cm	10 (20)
5-10 cm	16 (32)
>10 cm	24 (48)
Contour	
Round	4 (8)
Ovoid	4 (8)
Lobulated	42 (84)
Boundary	
Smooth	42 (84)
Irregular	0 (0)
Combined	8 (16)
Growth pattern	
Endoluminal	6 (12)
Exophytic	34 (68)
Mixed	10 (20)
Enhancement pattern	
Homogeneous	6 (12)
Heterogeneous	44 (88)
Degree of enhancement	
Poor	12 (24)
Moderate	32 (64)
Good	6 (12)
Necrosis	
Absent	8 (16)
Mild	9 (18)
Moderate	20 (40)
Severe	13 (26)
Calcification	7 (14)
Ulceration	20 (40)
Perilesional fat stranding	22 (44)
Adjacent organ invasion	9 (18)
Ascites	9 (18)
Lymphadenopathy	3 (6)
Bowel obstruction	1 (2)
Liver metastasis	10 (20)
Peritoneal seeding	8 (16)

GISTs = gastrointestinal stromal tumors

on portal venous phase and hyperattenuation on arterial phase.

Out of the 50 patients only the histology from surgical resections of 37 patients were used to evaluate the correlation between the mitotic rate and CT features because the histology from biopsy was insufficient to accurately count the mitosis in 50 high-power fields. Comparisons between the low and high mitotic rate groups on patient demographics, presenting symptom, tumor location, and CT characteristics were shown in Table 3. Twenty-four (65%) cases were classified as low mitotic rate (Fig. 4) and 13 (35%) as high mitotic rate (Fig. 5). The tumor sizes in the low mitotic rate group ranged from 1.2 to 16.6 cm (mean ± SD, 8.4±4.8 cm) and those of high mitotic rate group ranged from 3.1 to 18.3 cm (mean ± SD, 10.5±4.8 cm). One patient with liver metastasis had a 9.8-cm rectal GIST with a low mitotic rate. Tumor necrosis was found in all 13 patients with high mitotic rates. Peritoneal metastasis was noted in four patients with high mitotic rates, whereas none was noted in patients with low mitotic rates.

Size, boundary, degree of enhancement, necrosis, lymphadenopathy, liver metastasis, and peritoneal seeding showed some evidence of association (p<0.20) with high mitotic rate in univariate logistic analysis. Multivariate logistic regression analysis in which the model was refined by sequential removal of non-significant variables as indicated by the likelihood ratio test showed that only necrosis and peritoneal seeding were significant predictors of a high mitotic rate (p<0.05) (Table 4). By combination of these two variables, the probability and 95% confidence interval (CI) of a high mitotic rate varied from 0 (95% CI: 0, 0.41) in the absence of both variables to 0.35 (95% CI: 0.17, 0.56) in the presence of necrosis but absence of peritoneal seeding to 1 (95% CI: 0.40, 1.00)

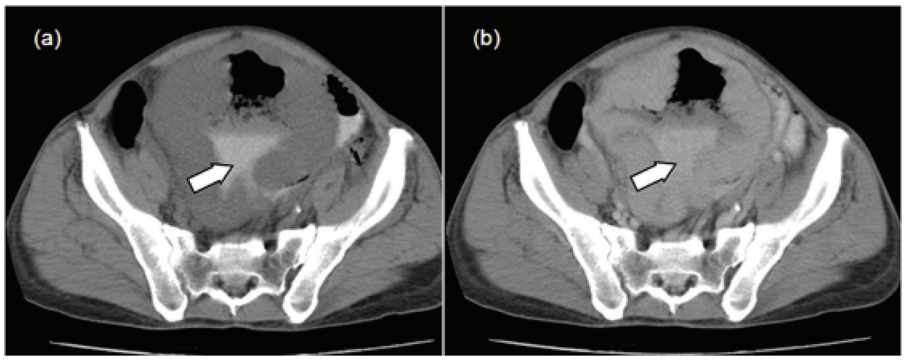

Fig. 2 A 58-year-old man with gastrointestinal stromal tumor of the small intestine presenting with abdominal pain. Computed tomography showed a large well-defined soft tissue mass in the pelvic cavity which was exophytic from the ileum and has ulceration (arrow): (a) non-enhanced; (b) contrast-enhanced.

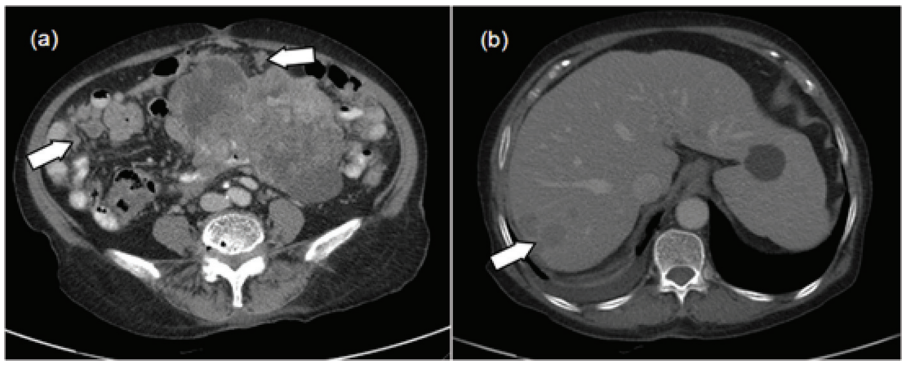

Fig. 3 An 82-year-old woman with malignant gastrointestinal stromal tumor of the small intestine presenting with abdominal pain. (a) Contrast-enhanced computed tomography obtained during portal venous phase shows a large heterogeneous mass with necrosis. Note small peritoneal metastases (arrows). (b) Contrast-enhanced computed tomography obtained during portal venous phase shows hypoattenuating metastatic nodules (arrow) in liver.

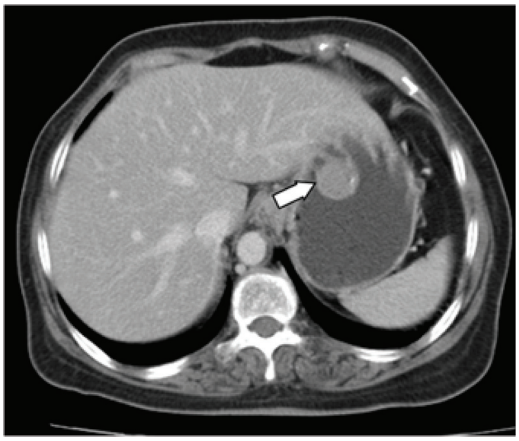

Fig. 4 A 67-year-old woman with benign gastrointestinal stromal tumor of the stomach presenting with abdominal pain. Contrast-enhanced computed tomography showed a well-defined endoluminal gastric tumor (arrow).

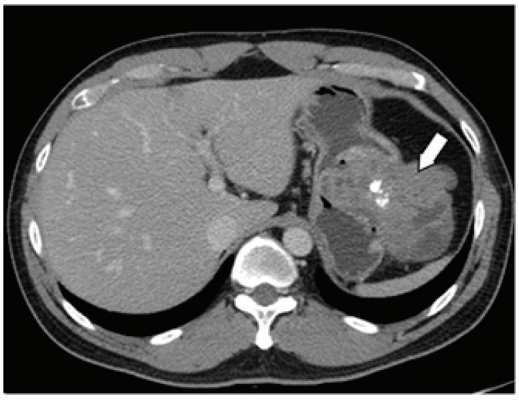

Fig. 5 A 40-year-old man with malignant gastrointestinal stromal tumor of the stomach presented with gastrointestinal bleeding. Contrast-enhanced computed tomography showed a well-defined dumbbell-shaped tumor (arrow) with necrosis, ulceration and calcifications.

Table 3. Patient demographic data, presenting symptoms, locations, and CT characteristics

	Low mitotic rate (n, %) (total n = 24)	High mitotic rate (n, %) (total n = 13)	*p*-value
Demographic data			
Gender			0.491
Male	11 (73)	4 (27)	
Female	13 (59)	9 (41)	
Age (year), mean ± SD	60±8	57±17	0.540
Presenting symptom			0.538
Symptomatic	21 (62)	13 (38)	
Asymptomatic	3 (100)	0 (0)	
Lesion location			1.000
Stomach	15 (63)	9 (37)	
Small bowel	8 (67)	4 (33)	
Rectum	1 (100)	0 (0)	
CT characteristics			
Size			0.185
≤5 cm	8 (89)	1 (11)	
5-10 cm	7 (50)	7 (50)	
>10 cm	9 (64)	5 (36)	
Contour			0.374
Round	4 (100)	0 (0)	
Ovoid	2 (67)	1 (33)	
Lobulated	18 (60)	12 (40)	
Boundary			0.140
Smooth	19 (59)	13 (41)	
Irregular	0 (0)	0 (0)	
Combined	5 (100)	0 (0)	
Growth pattern			0.474
Endoluminal	4 (80)	1 (20)	
Exophytic	13 (57)	10 (43)	
Mixed	7 (78)	2 (22)	
Enhancement pattern			0.638
Homogeneous	4 (80)	1 (20)	
Heterogeneous	20 (63)	12 (37)	
Degree of enhancement			0.132
Poor	6 (67)	3 (33)	
Moderate	12 (55)	10 (45)	
Good	6 (100)	0 (0)	
Necrosis			0.022
Absent	7 (100)	0 (0)	
Mild	2 (25)	6 (75)	
Moderate	9 (64)	5 (36)	
Severe	6 (75)	2 (25)	
Calcification			1.000
Absent	20 (65)	11 (35)	
Present	4 (67)	2 (33)	
Ulceration			0.472
Absent	17 (71)	7 (29)	
Present	7 (54)	6 (46)	
Perilesional fat stranding			1.000
Absent	16 (67)	8 (33)	
Present	8 (62)	5 (38)	
Adjacent organ invasion			0.278
Absent	23 (68)	11 (32)	
Present	1 (33)	2 (67)	
Ascites			0.321
Absent	22 (69)	10 (31)	
Present	2 (40)	3 (60)	
Lymphadenopathy			0.117
Absent	24 (69)	11 (31)	
Present	0 (0)	2 (100)	
Bowel obstruction			-
Absent	24 (65)	13 (35)	
Present	0 (0)	0 (0)	
Liver metastasis			0.115
Absent	23 (70)	10 (30)	
Present	1 (25)	3 (75)	
Peritoneal seeding			0.011
Absent	24 (73)	9 (27)	
Present	0 (0)	4 (100)	

Table 4. Numbers of patients with low and high mitotic rates according to each combination of necrosis and peritoneal seeding

Necrosis	Peritoneal seeding	Mitotic rate		Total	Probability (95% CI)
		Low	High		
Absent	Absent	7	0	7	0 (0, 0.41)
Present	Absent	17	9	26	0.35 (0.17, 0.56)
Present	Present	0	4	4	1.00 (0.40, 1.00)
Total		24	13	37	0.35 (0.20, 0.53)

Table 5. Logistic regression model to predict high mitotic rate using the bias-reduction model of Firth 1993

Necrosis	Peritoneal seeding	OR (95% CI)	*p*-value
Absent	Absent	1	0.006
Present	Absent	8.14 (0.83, 1,100)	
Present	Present	135 (5.1, 45,000)	

in the presence of both (Table 4). The combination variable logistic regression model using the bias-reduction model of Firth result was shown in Table 5. There was strong evidence that the combination of presence of necrosis and peritoneal seeding can predict high mitotic rate.

Discussion

In the present study, the authors found that GISTs showed several common CT characteristics. They were usually lobulated, smooth marginated masses that were predominantly exophytic and had heterogeneous enhancement with areas of necrosis. Ulceration and perilesional fat stranding were sometimes demonstrated. Calcification in the tumor was an uncommon finding. Lymphadenopathy and gut obstruction were rarely noted and they were probably not features of GISTs. The present findings were similar to those of previous studies[7,9,12].

The liver is the most common site of GIST metastasis, followed by the peritoneum[20]. The CT characteristics of metastasis within the liver are similar to those of primary tumors; a hyperattenuating or hypervascular enhancing mass that can be a heterogeneous enhancement due to necrosis, hemorrhage or cystic degeneration[21], which is usually hypoattenuating on portal venous phase[9]. In present series, most of hepatic metastatic nodules in nine patients showed this appearance except for two nodules in one patient that showed isoattenuation on portal venous phase and hyperattenuation on arterial phase. The authors probably missed some hypervascular liver metastases because only 26 in 50 patients underwent biphasic CT scans. Arterial phase CT scan is important in evaluation of hypervascular liver metastasis of GISTs.

Although some previous studies showed that GISTs have a male predominance[6,9,10], the present study as well as others showed no gender predilection[11-13]. The most common presenting symptom of GISTs in our series was gastrointestinal bleeding. This result was consistent with previous reports[6,7,13]. Patients may present with hematemesis, melena, hematochezia, or signs and symptoms of anemia. Other common presenting symptoms are abdominal pain or palpable mass. In other reports, abdominal pain was the most common presenting symptom[11,12].

In multivariate analysis, the present study showed that the presence of necrosis and peritoneal seeding were significant independent predictors of high mitotic rate. Our results seem to differ from those of other studies using multivariate analysis[11-13]. Tateishi et al[11], using multiple stepwise logistic regression, reported that extrinsic epicenter and unclear boundary were the most significant predictors of high-grade GIST, while Kim et al[12] and Yang et al[13] found that tumor size was the only significant predictive factor for high mitotic rate or malignant GIST. This discrepancy may be explained by different histologic grading criteria for classification of benign and malignant or low grade and high grade GIST. Tateishi et al[11] used the MIB-1 score and classified tumors as low grade or high grade. There were no clear histologic criteria for grading in Yang's study[13]. Kim et al[12] used the same histologic criteria as our study but their cases were limited to tumors of gastric origin.

The combined presence of both necrosis and peritoneal seeding, indicated a high probability of high mitotic rate (1, 95% CI = 0.40, 1.0) and the absence of

both indicated a low probability of high mitotic rate (0, 95% CI = 0, 0.41). Tumors that show low mitotic count (≤5 mitoses per 50 HPF) usually have a benign behavior. However, a low mitotic count does not always rule out malignant behavior that can metastasize[15,22]. There was one rectal GIST patient in present study who had a low mitotic rate but with liver metastasis. Besides mitotic count, size of the tumor is another important morphologic criterion for prediction of tumor behavior and the significance of size is site dependent. Specifically, gastric GISTs seem to behave less aggressively than intestinal tumors[23]. Most proposed criteria for evaluation of GIST malignant potential were comprised of mitotic rate, size, and site[15-19]. Therefore, prediction of mitotic rate from CT features indirectly helps to predict malignancy since tumor size and site can be evaluated by CT scan.

The present study had numbers of limitation. This was a retrospective study of collected cases over a period of years at a tertiary hospital and the number of patients was small. The authors were unable to collect the hard copy of CT images of patients referred from other hospitals. Moreover, there were variations in CT equipment and imaging techniques. A prospective multicenter study of a large number of patients would be more decisive.

In conclusion, the typical CT features of GISTs are lobulated, smooth marginated masses that are predominantly exophytic and have heterogeneous enhancement with areas of necrosis. Ulceration and perilesional fat stranding are sometimes demonstrated. Calcification, lymphadenopathy and gut obstruction are uncommon finding. Moreover, the authors observed that the presence of both necrosis and peritoneal seeding are significant predictor of high mitotic rate of GISTs when compared with their absence. The probability of a high mitotic rate was 1 (95% CI: 0.40-1.00).

What is already known on this topic?

Gastrointestinal stromal tumors (GISTs) are the most common mesenchymal neoplasms of the gastrointestinal tumors and positive expression of KIT (CD117) is the best diagnostic tool of this tumor. The computed tomographic findings of GISTs have been previously described in the literature and showed some distinctive features that help differentiate them from epithelial neoplasms. A few studies have attempted to correlate CT features with the histologic grading or prediction of malignancy but they have still produced conflicting results.

What this study adds?

This study showed characteristic computed tomographic findings of GISTs. The presence of both necrosis and peritoneal seeding in computed tomography is a significant predictor of high mitotic rate of GISTs.

Acknowledgements

The authors wish to thank Dr. Alan Geater for the statistical analysis.

Potential conflicts of interest

None.

References

1. Mazur MT, Clark HB. Gastric stromal tumors. Reappraisal of histogenesis. Am J Surg Pathol 1983; 7: 507-19.
2. Appelman HD. Mesenchymal tumors of the gut: historical perspectives, new approaches, new results, and does it make any difference? Monogr Pathol 1990; 220-46.
3. Kitamura Y, Hirota S, Nishida T. Molecular pathology of c-kit proto-oncogene and development of gastrointestinal stromal tumors. Ann Chir Gynaecol 1998; 87: 282-6.
4. Kindblom LG, Remotti HE, Aldenborg F, Meis-Kindblom JM. Gastrointestinal pacemaker cell tumor (GIPACT): gastrointestinal stromal tumors show phenotypic characteristics of the interstitial cells of Cajal. Am J Pathol 1998; 152: 1259-69.
5. Strickland L, Letson GD, Muro-Cacho CA. Gastrointestinal stromal tumors. Cancer Control 2001; 8: 252-61.
6. Chamadol N, Laopaiboon V, Promsorn J, Bhudhisawasd V, Pagkhem A, Pairojkul C. Gastrointestinal stromal tumor: computed tomographic features. J Med Assoc Thai 2009; 92: 1213-9.
7. Levy AD, Remotti HE, Thompson WM, Sobin LH, Miettinen M. Gastrointestinal stromal tumors: radiologic features with pathologic correlation. Radiographics 2003; 23: 283-304.
8. Sandrasegaran K, Rajesh A, Rushing DA, Rydberg J, Akisik FM, Henley JD. Gastrointestinal stromal tumors: CT and MRI findings. Eur Radiol 2005; 15: 1407-14.
9. Burkill GJ, Badran M, Al Muderis O, Meirion TJ, Judson IR, Fisher C, et al. Malignant gastrointestinal stromal tumor: distribution, imaging features, and

pattern of metastatic spread. Radiology 2003; 226: 527-32.
10. Ghanem N, Altehoefer C, Furtwangler A, Winterer J, Schafer O, Springer O, et al. Computed tomography in gastrointestinal stromal tumors. Eur Radiol 2003; 13: 1669-78.
11. Tateishi U, Hasegawa T, Satake M, Moriyama N. Gastrointestinal stromal tumor. Correlation of computed tomography findings with tumor grade and mortality. J Comput Assist Tomogr 2003; 27: 792-8.
12. Kim HC, Lee JM, Kim KW, Park SH, Kim SH, Lee JY, et al. Gastrointestinal stromal tumors of the stomach: CT findings and prediction of malignancy. AJR Am J Roentgenol 2004; 183: 893-8.
13. Yang TH, Hwang JI, Yang MS, Hung SW, Chan SW, Wang J, et al. Gastrointestinal stromal tumors: computed tomographic features and prediction of malignant risk from computed tomographic imaging. J Chin Med Assoc 2007; 70: 367-73.
14. Ulusan S, Koc Z, Kayaselcuk F. Gastrointestinal stromal tumours: CT findings. Br J Radiol 2008; 81: 618-23.
15. Fletcher CD, Berman JJ, Corless C, Gorstein F, Lasota J, Longley BJ, et al. Diagnosis of gastrointestinal stromal tumors: A consensus approach. Hum Pathol 2002; 33: 459-65.
16. Miettinen M, El Rifai W, Sobin HL, Lasota J. Evaluation of malignancy and prognosis of gastrointestinal stromal tumors: a review. Hum Pathol 2002; 33: 478-83.
17. Huang HY, Li CF, Huang WW, Hu TH, Lin CN, Uen YH, et al. A modification of NIH consensus criteria to better distinguish the highly lethal subset of primary localized gastrointestinal stromal tumors: a subdivision of the original high-risk group on the basis of outcome. Surgery 2007; 141: 748-56.
18. Goh BK, Chow PK, Yap WM, Kesavan SM, Song IC, Paul PG, et al. Which is the optimal risk stratification system for surgically treated localized primary GIST? Comparison of three contemporary prognostic criteria in 171 tumors and a proposal for a modified Armed Forces Institute of Pathology risk criteria. Ann Surg Oncol 2008; 15: 2153-63.
19. Demetri GD, Benjamin RS, Blanke CD, Blay JY, Casali P, Choi H, et al. NCCN Task Force report: management of patients with gastrointestinal stromal tumor (GIST)--update of the NCCN clinical practice guidelines. J Natl Compr Canc Netw 2007; 5 (Suppl 2): S1-29.
20. Horton KM, Juluru K, Montogomery E, Fishman EK. Computed tomography imaging of gastrointestinal stromal tumors with pathology correlation. J Comput Assist Tomogr 2004; 28: 811-7.
21. Hong X, Choi H, Loyer EM, Benjamin RS, Trent JC, Charnsangavej C. Gastrointestinal stromal tumor: role of CT in diagnosis and in response evaluation and surveillance after treatment with imatinib. Radiographics 2006; 26: 481-95.
22. Miettinen M, Lasota J. Gastrointestinal stromal tumors--definition, clinical, histological, immunohistochemical, and molecular genetic features and differential diagnosis. Virchows Arch 2001; 438: 1-12.
23. Emory TS, Sobin LH, Lukes L, Lee DH, O'Leary TJ. Prognosis of gastrointestinal smooth-muscle (stromal) tumors: dependence on anatomic site. Am J Surg Pathol 1999; 23: 82-7.

ลักษณะภาพรังสีส่วนตัดอาศัยคอมพิวเตอร์ของ GIST และการหาลักษณะภาพที่ช่วยบ่งชี้ GIST แบบร้ายแรง

ศิริพร พินัยกุล, ปิยนุช วุฒิชาติปรีชา, สมรมาศ กันเงิน, สมบัติ ลีลาเกียรติไพบูลย์

วัตถุประสงค์: เพื่อศึกษาลักษณะภาพรังสีส่วนตัดอาศัยคอมพิวเตอร์ของ GIST และวิเคราะห์หาลักษณะภาพที่เป็นตัวทำนาย GIST แบบร้ายแรง

วัสดุและวิธีการ: เป็นการศึกษาแบบย้อนหลัง โดยรังสีแพทย์ 2 คน แปลผลภาพรังสีส่วนตัดอาศัยคอมพิวเตอร์ของผู้ป่วย 50 ราย ที่ได้รับการวินิจฉัยทางพยาธิวิทยาว่าเป็น GIST และการตีความขั้นสุดท้ายใช้การเห็นพ้องต้องกันของทั้งสองคน ลักษณะภาพรังสีส่วนตัดอาศัยคอมพิวเตอร์ที่ศึกษาคือ ตำแหน่ง ขนาด รูปร่าง ขอบนอก แบบอย่างการเติบโต แบบอย่างและระดับของ enhancement การตายเฉพาะส่วนของก้อน การมีแคลเซียมเกาะ แผล stranding ของไขมันรอบรอยโรค ภาวะลำไส้อุดกั้น และสิ่งแสดงเนื้อร้าย แต่ละลักษณะจะถูกเปรียบเทียบ โดยใช้การทดสอบ Fisher's exact หรือ t-test รวมทั้งหาลักษณะภาพที่เป็นตัวทำนายอัตรากระบวนการแบ่งเซลล์สูงโดยใช้ univariate และ multivariate logistic regression

ผลการศึกษา: จากผู้ป่วย 50 ราย กระเพาะอาหารเป็นตำแหน่งที่พบ GIST มากที่สุด คือ 62% ขนาดเฉลี่ย 10.2 เซนติเมตร (ค่าเบี่ยงเบนมาตรฐาน 5.2 เซนติเมตร) รูปร่างเป็นกลีบย่อย 84% ขอบเรียบ 84% แบบอย่างการเติบโตแบบ exophytic 68% ก้อนส่วนมากมีความหนาแน่นที่ไม่เป็นเนื้อเดียวกันหลังฉีดสารเพิ่มความชัดภาพ 88% พบการตายเฉพาะส่วน 84% การมีแคลเซียมเกาะ 14% แผล 40% strandingของไขมันรอบรอยโรค 44% ภาวะลำไส้อุดกั้น 2% มีการบุกรุกไปอวัยวะข้างเคียง 18% ท้องมาน 18% โรคปุ่มน้ำเหลือง 6% แพร่กระจายไปที่ตับ 20% และแพร่กระจายไปที่เยื่อบุช่องท้อง 16% การตายเฉพาะส่วนและการแพร่กระจายไปที่เยื่อบุช่องท้องเป็นตัวทำนายก้อนเนื้อที่มีอัตรากระบวนการแบ่งเซลล์สูงใน multivariate logistic regression อย่างมีนัยสำคัญทางสถิติ ($p<0.05$) ถ้ามีร่วมกันทั้งสองลักษณะนี้จะมีความน่าจะเป็นเท่ากับ 1 (95% CI, 0.40-1.00)

สรุป: กระเพาะอาหารเป็นตำแหน่งที่พบ GIST มากที่สุด ลักษณะภาพรังสีส่วนตัดอาศัยคอมพิวเตอร์ที่พบบ่อยคือ รูปร่างเป็นกลีบย่อย ขอบเรียบ แบบอย่างการเติบโตแบบ exophytic และมีความหนาแน่นที่ไม่เป็นเนื้อเดียวกันหลังฉีดสารเพิ่มความชัดภาพ การพบการตายเฉพาะส่วนและการแพร่กระจายไปที่เยื่อบุช่องท้องร่วมกันเป็นตัวทำนายที่มีนัยสำคัญของก้อนเนื้อที่มีอัตรากระบวนการแบ่งเซลล์สูง โดยมีความน่าจะเป็นเท่ากับ 1 (95% CI, 0.40-1.00)